ORIGINAL ARTICLE

CrossMark

Cyclin-dependent kinase inhibitors, roscovitine and purvalanol, induce apoptosis and autophagy related to unfolded protein response in HeLa cervical cancer cells

Pelin Ozfiliz-Kilbas[1] · Bahar Sarikaya[1] · Pinar Obakan-Yerlikaya[1] · Ajda Coker-Gurkan[1] · Elif Damla Arisan[1] · Benan Temizci[1] · Narcin Palavan-Unsal[1]

Abstract

Roscovitine (Rosc) and purvalanol (Pur) are competitive inhibitors of cyclin-dependent kinases (CDKs) by targeting their ATP-binding pockets. Both drugs are shown to be effective to decrease cell viability and dysregulate the ratio of pro- and anti-apoptotic Bcl-2 family members, which finally led to apoptotic cell death in different cancer cell lines in vitro. It was well established that Bcl-2 family members have distinct roles in the regulation of other cellular processes such as endoplasmic reticulum (ER) stress. The induction of ER stress has been shown to play critical role in cell death/survival decision via autophagy or apoptosis. In this study, our aim was to investigate the molecular targets of CDK inhibitors on ER stress mechanism related to distinct cell death types in time-dependent manner in HeLa cervical cancer cells. Our results showed that Rosc and Pur decreased the cell viability, cell growth and colony formation, induced ER stress-mediated autophagy or apoptosis in time-dependent manner. Thus, we conclude that exposure of cells to CDK inhibitors induces unfolded protein response and ER stress leading to autophagy and apoptosis processes in HeLa cervical cancer cells.

Keywords Roscovitine · Purvalanol · Cervical cancer · ER stress · Autophagy · Apoptosis

✉ Pinar Obakan-Yerlikaya
   p.obakan@iku.edu.tr

   Pelin Ozfiliz-Kilbas
   p.ozfiliz@iku.edu.tr

   Bahar Sarikaya
   1302060029@stu.iku.edu.tr

   Ajda Coker-Gurkan
   a.coker@iku.edu.tr

   Elif Damla Arisan
   d.arisan@iku.edu.tr

   Benan Temizci
   temizci@itu.edu.tr

   Narcin Palavan-Unsal
   n.palavanunsal@iku.edu.tr

[1] Department of Molecular Biology and Genetics, Istanbul Kultur University, Atakoy Campus, 34156 Istanbul, Turkey

Introduction

Cervical cancer is the fourth common cancer type among women following human papillomavirus (HPV) infection worldwide. There are several methods for the treatment of cervical cancer cases including radiation therapy alone or in combination with several anti-mitotic or anti-proliferative chemotherapeutic agents [1]. CDKs are important kinase family members regulating cell cycle machinery with their counterparts, cyclins [2]. Deregulation of cell cycle progression could activate malign cell turnover, which cause progressive cancer development. For this reason, highly potent CDK inhibitors gain importance in cancer therapy due to their high apoptotic potential in proliferating cells [3]. Rosc (Roscovitine, also known as CYC202 and Seliciclib) is one of the well-established CDK inhibitors, which induces apoptosis in HeLa cervical cancer cells. In addition, exposure of cells to Rosc inhibited cell survival and induced cell cycle arrest at G1/S or G2/M transition [4]. In addition, Rosc has been also suggested as an autophagy inducing agent through modulating biomarkers of autophagy [5–7]. In glioblastoma cancer cells, it was shown that Rosc

treatment induced apoptosis through inhibited CDK2, 7, 9 and cyclin A, D and E counterparts [8]. In HeLa cervical cancer cells, Rosc decreased cell viability and triggered autophagic or apoptotic processes according to the early and late time treatments [6]. Similar CDK1, CDK2, CDK5, CDK7 and CDK9 inhibition and p53-dependent DNA damage were shown in Rosc-treated head and neck cancer cells [9]. In breast cancer cells, time-dependent treatment of Rosc revealed a significant inhibition on cell proliferation depending on estrogen receptor α status. Pur is a new generation CDK inhibitor, which exerts its function through blocking the binding of CDK1 or CDK2 with their specific cyclin counterparts and targets cell cycle arrest at G1/S or G2/M phases and apoptotic induction in caspase-dependent manner. Concomitantly, it was shown that Pur treatment caused the downregulation of anti-apoptotic Bcl-2 and survivin. In addition, Pur was also found effective to induce endoplasmic reticulum (ER) stress in HCT 116 colon cancer cells [10, 11]. In breast cancer cells, Pur also induced caspase-dependent apoptosis depending on their estrogen receptor status [9]. Pur has been shown to cause cell cycle arrest and endoplasmic reticulum-mediated apoptosis in colon cancer cells. In addition, different cell death mechanisms were also found associated with time-dependent Pur treatment in colon cancer cell lines. On the other hand, co-treatment of either Rosc or Pur with rapamycin, the well-known mTOR (mammalian target of rapamycin) inhibitor, further increased apoptosis in DU145 and LNCaP prostate cancer cells depending on their androgen receptor expression levels through suppressing PI3K/AKT/mTOR pathway [12]. Although, both Rosc and Pur are strong apoptotic inducers, the mechanistic action of these CDK inhibitors in other cell death related signaling cascades are not fully understood.

ER is the organelle responsible for regulation of functional protein maintenance such as folding, maturation, translocation, degradation and post-translational modifications. Impaired ER functions caused failure of protein synthesis or transport and Ca^{2+} overload [13]. During ER stress, unfolded protein response (UPR) could be activated to regulate protein homeostasis via ER-associated degradation process (ERAD) or apoptotic cell death to overcome dysregulated proteins. During UPR, three ER transmembrane receptors; Protein kinase RNA-like ER kinase (PERK), Inositol-requiring Enzyme 1α (IRE1α) and Activating transcription factor 6 (ATF6) can be activated by the disassociation of the stress sensor molecule Glucose-regulated protein/binding immunoglobulin protein (GRP78/BiP). PERK is a transcriptional regulator which inhibits the accumulation of newly-synthesized proteins in ER lumen by phosphorylating Eukaryotic Translation Initiation Factor 2 (eIF2α) [14]. The phospho-eIF2α led to activation of UPR-dependent genes such as Activating transcription factor 4 (ATF4) and transcriptional factor C/

EBP homologous protein (CHOP). The second ER membrane-resident receptor IRE1α has an endonuclease activity on X-box binding protein 1 (XBP1) mRNA leading to removal of its 26 nucleotide intron and creates a splice variant. This mature form of XBP1 is a transcription factor for ER chaperones genes such as calreticulin (CALR), protein disulphite isomerase (PDI), p58, DnaJ, etc [15]. IRE1α, apart from XBP1 activation, might also induce the stress response regulator protein, c-Jun N-terminal kinase (JNK) resulting the upregulation of certain pro-apoptotic proteins such as Bim, Bid, and Bax [16]. The latter receptor in ER membrane, ATF6, serves as a transcription factor for CHOP, BiP, XBP1 and PDI.

Autophagy is the degradation process of aged or nonfunctional cytoplasmic components or mis/unfolded proteins within autophagosomes following lysosomal fusion step [17, 18]. Recent studies revealed distinct functions of autophagy in physiological and pathophysiological conditions such as cell death or survival, starvation adaptation, anti-aging, development, microorganism elimination. Several proteins including Ulk1/2 complex and mTOR control autophagy initiation process via induction of autophagosome formation through Autophagy-related genes (Atgs), Beclin-1 and its inhibitory binding partner Bcl-2 or Bcl-x_L. Phagophore formation and maturation could be determined by LC3 and SQSTM1/p62, the autophagy regulating molecules sequestered in the vesicles and degraded [14].

Autophagy activating conditions such as starvation, UPR and other stress conditions inhibit mTOR via Akt signaling, and activate Ulk1/2 complex, which in turn facilitates autophagosome formation via modulated expression levels of ATG proteins and Beclin-1. The phosphorylation of Akt via phosphoinositide-dependent kinase 1 (PDK1) leads to the inhibition of TSC2 (tuberous sclerosis complex 2), which forms a complex with TSC1 and together they are a critical negative regulator of mTOR [19]. Phosphorylation of Akt at Ser 241 residue lead to regulation of energy metabolism to maintain cell survival in the cancer cells [20].

Autophagy has been reported to either inhibit or promote cancer cell survival depending on the stress level. ER stress has been shown to be dynamically connected to autophagy and apoptosis. Moderate ER stress was shown to induce autophagy to degrade mis/unfolded proteins and increase chaperone transcription [14]. However, severe ER stress was found related to the induction of apoptotic cell death [21–23]. Consequently, ER stress is a very critical process in the response of cells against cancer chemotherapy.

In this study, our aim was to determine the potential effect of CDK inhibitors on ER stress players in autophagy and apoptosis decision of HeLa cervical cancer cells. Our findings suggested that ER stress is induced in both early and late times of CDK inhibitors exposure to HeLa cells leading autophagy and apoptosis.

Materials and methods

Drugs, antibodies and chemicals

Rosc and Pur which were used as CDK inhibitors were purchased from Tocris Bioscience (Bristol, UK). They were dissolved in DMSO and 10 mM stocks were prepared and stored at -20 °C. All primary and secondary antibodies were purchased from Cell Signaling Technology (CST, Danvers, MA, USA).

Cell culture

HeLa cervical cancer cells (CCL-2) were purchased from the American Type Culture Collection (ATCC, Manassas, VA, USA) and were maintained in DMEM (Gibco-Life Technologies, CA, USA) with 10% fetal bovine serum (Pan Biotech, Aidenbach, Germany) and 100 U/100 mg/ml penicillin/streptomycin (PAN Biotech, Aidenbach, Germany) in humidified incubator at 37 °C with 5% CO_2. (Heracell 150; Thermo Electron Corporation, Waltham, MA, USA).

MTT cell viability assay

The cytotoxic effects of Rosc and Pur on HeLa cell viability were determined by colorimetric MTT 3-(4,5-dimethylthiazol-2-yl)-2,5-diphenyl-tetrazolium bromide (MTT; Roche, Indianapolis, IN, USA) assay. For this purpose, HeLa cells were seeded at 8×10^3 cells/well in 96-well plates and were kept in incubator overnight for their attachment. Then, cells were treated with Rosc and Pur (0–75 µM) in time-dependent manner. After Rosc or Pur treatment, 10 µl of MTT reagent (5 mg/ml) was added to the cell culture medium for 4 h. Meanwhile, formazan crystals were generated due to mitochondria activation. Then, cell culture medium was removed and 200 µl DMSO was added to wells for dissolving the formazan crystals. The absorbance was determined at 570 nm with a microplate reader (Bio-Rad, Hercules, CA, USA).

Survival assay (Trypan blue dye exclusion assay)

Cells were seeded at 1×10^5 cells per well in six-well plates and treated with Rosc (20 µM) or Pur (10 µM) for 24, 48 and 72 h. According to the time points, cells were trypsinized and counted by using 0.4 (w/v) trypan blue dye at 1:1 ratio. 10 µl of cells were counted by dual-chamber Neubauer haemocytometer under light microscopy. Data

were platted on graph indicating the number of cells (y-axis) vs. time (x-axis).

Colony formation assay

To understand the effect of Rosc and Pur on colony formation, HeLa cells were seeded at 600 cells per well in 6-well plates and incubated in the presence or absence of CDK inhibitors for 14 days. After this time period, media was removed and cells were washed with 1× PBS, fixed with methanol:acetic acid (3:1) for 5 min. After removal of fixing agent, cells were stained with 0.5% crystal violet in methanol for 15 min, then cells were washed by distilled water, and the morphological images were taken under light microscopy.

Fluorescence microscopy

PI staining

HeLa cells were seeded at 5×10^4 cells per 12-well plates and treated with Rosc (20 µM) and Pur (10 µM) for 4, 12, 24 and 48 h. Through Rosc and Pur treatment, HeLa cells were washed with 1× PBS and propidium iodide (PI) was performed to cells (50 mg/ml stock concentration in 1× PBS) and incubated for 30 min in the incubator. Dead cells (red stained cells) which were occurred through drug treatment was determined by fluorescence microscopy in excitation 535 nm and emission 617 nm (Olympus, Tokyo, Japan).

DAPI staining

Cells were treated with Rosc (20 µM) and Pur (10 µM) for 24 and 48 h. Following drug treatment, cells washed with 1× PBS. 1 µl/ml 4′,6-diamidino-2-phenylindole (DAPI) (1 mg/ml stock concentration in 1× PBS) was performed for 10 min in the dark. Nuclear fragmentation (blue stained cells) due to drug treatment was determined by fluorescence microscopy in excitation 358 nm and emission 461 nm (Olympus, Tokyo, Japan).

DiOC6 staining

HeLa cells were seeded at 5×10^4 density into 12-well plate/per well. Following exposure of cells to Rosc (20 µM) and Pur (10 µM), they were washed with 1× PBS, and stained with 4 nM 3,3′-dihexyloxacarbocyanine iodide (DiOC6) (40 nM stock concentration in DMSO; Calbiochem, La Jolla, CA, USA) for 15 min in dark. Mitochondrial membrane potential (MMP) disruption was determined by fluorescence microscopy in excitation 482 nm and emission 504 nm (Olympus, Tokyo, Japan).

FACS flow cytometry experiments

Cell cycle distribution by PI staining

HeLa cells were seeded in 6-well plates at a density 2×10^5 cells/well and treated with Rosc (20 µM) and Pur (10 µM) for 4, 12, 24 and 48 h, respectively. Then cells were trypsinized, washed with 1× PBS, centrifuged at 2000×g rpm for 5 min and fixed with 70% ethanol overnight at 4 °C. Then cells were centrifuged again, supernatant was removed and cells were stained with 10 µl of 40 µg/µl PI with 50 µl of 20 µg/ml RNase at 37 °C for 30 min in the dark. 10,000 cells per sample were analyzed by flow cytometer. The cell cycle distribution was determined by Accuri C6 (BD Biosciences, Oxford, UK) and data analyses was performed BD Accuri C6 software (BD Biosciences).

Apoptosis determination by Annexin V/PI staining

HeLa cells were seeded at 2×10^5 cells/well density in 6-well plates and treated with Rosc (20 µM) and Pur (10 µM) for 12, 24 and 48 h. They were trypsinized, washed with 1× PBS, centrifuged at 2000×g rpm for 5 min and then Annexin V/PI staining was performed according to the manufacturer's instructions FITC Annexin V Apoptosis Detection Kit I, (BD Biosciences, Oxford, UK). The apoptosis was determined by Accuri C6 (BD Biosciences, Oxford, UK) and data analyses was performed using BD Accuri C6 software (BD Biosciences).

Determination of ROS generation

Intracellular reactive oxygen species (ROS) were determined by FACS flow analysis after cell labeling with DCFH-DA (7′-dichlorodihydrofluorescein diacetate). DCFH-DA is a non-fluorescent molecule, but once it enters into cells, it is deacetylated by cellular esterases and rapidly oxidized to highly fluorescent DCF (2′,7′-dichlorodihydrofluorescein) by ROS. The observed fluorescence intensity is directly proportional to intracellular ROS levels. After treatment procedure, cells were stained with DCFH-DA (1 µM final concentration) and incubated for 10 min at 37 °C, washed with 1X PBS and then analyzed by a Accuri C6 (BD Biosciences, Oxford, UK) and data analyses was performed by BD Accuri C6 software (BD Biosciences) (Excitation/Emission: 495/529 nm).

CHOP activation determination by pmCherry-1 plasmid transfection

Cells were seeded in 6-well plates and transfected with the reporter construct CHOP promoter (−649/+136) pmCherry-1 plasmid (0.5 mg/ml) (Addgene plasmid #36035) using the Fugene 6 according to the manufacturer's instructions (Promega, Sunnyvale, CA, USA). After a 24 h transfection, cells were exposed to Rosc (20 µM) and Pur (10 µM) for 15′,30′, 1, 2, 4 h. Following drug treatment, mCherry-CHOP plasmid-transfected 1×10^4 cells/sample were determined by Accuri C6 (BD Biosciences, Oxford, UK) and data analyses was performed by BD Accuri C6 software (BD Biosciences, Oxford, UK) (Excitation/Emission: 587/610 nm).

Protein extraction and immunoblotting

HeLa cells were treated with Rosc (20 µM) and Pur (10 µM) in a time-dependent manner. Samples were washed with ice cold 1X PBS and lysed on ice with M-PER™ Mammalian Protein Extraction Reagent (Thermo Scientific, Rockford, IL, USA) and protease inhibitor cocktail (Roche, Mannheim, Germany) and centrifuged for 20′ at 13,200×g rpm. Protein concentrations were determined by the Bradford protein assay (Bio-Rad, Hercules, CA, USA). 30 µg total protein was separated on a 12% SDS-PAGE and transferred onto PVDF membranes (Roche, Mannheim, Germany). The membranes were then blocked with 5% milk blocking solution in Tris buffer saline (TBS)-Tween 20 (Sigma-Aldrich, St. Louis, MO, USA) and incubated with primary and horseradish peroxidase (HRP)-conjugated secondary antibodies (CST, Danvers, MA, USA) in 5% (v/v) milk blocking solution. Following the addition of enhanced chemiluminescence reagent, signals from the HRP-coupled antibodies were detected using ChemiDoc MP Imaging System (Bio-Rad Laboratories, Hercules, CA). All results were replicated at least three times and representative blots were given.

Statistical analysis

The statistical analyses of all the experiments were performed by two way ANOVA using GraphPad Prism 7.00 for Windows, GraphPad Software, La Jolla California USA, http://www.graphpad.com. Error bars were obtained from the ± standard deviation (SD) of three replicate experiments.

Results

CDK inhibitors decreased cell viability and survival ratio of HeLa cervical cells in time-dependent manner

Cells were incubated with various doses (0–75 µM) of each CDK inhibitors for 24 and 48 h and cell viability was determined by MTT assay. Both CDK inhibitors induced cell viability loss in dose- and time-dependent manner in HeLa cells. 20 µM Rosc and 10 µM Pur decreased cell viability by

25% within 24 h (Fig. 1a). The same doses were used in a time dependent-manner (0–72 h) for trypan blue dye exclusion assay. Both CDK inhibitors were able to inhibit cell survival starting from 24 h significantly (Fig. 1b). We demonstrated that Rosc and Pur are moderate cytotoxic agents for HeLa cells at selected 20 and 10 µM doses, respectively. We continued with these doses which cause 25% reduction in the cell viability for further experiments, instead of IC50 values, to understand the ability of drugs to trigger different signaling pathways in low doses. Since the moderate cytotoxic concentrations were tested in our previous studies and are known to induce apoptotic cell death, even necrosis in different cell lines such as HCT 116 colon cancer cells [24] .

We next tested the effect of each drug on colony forming potential of HeLa cells. Rosc and Pur at these concentrations significantly inhibited clonogenic survival of

HeLa cells more significantly at 24 h for Rosc and 48 h for Pur (Fig. 1c). The rate of the colony formation was calculated according to pixel analysis using ImageJ software. Our results indicated that both CDK inhibitors were able to diminish colony formation significantly after 24 and 48 h treatment (Fig. 1c, right panel).

CDK inhibitors treatment induced cell death, which was determined following PI staining by fluorescence microscopy. PI positive dead cells (red stained cells) augmented in a time-dependent manner following drug treatment within 48 h (Fig. 1d). PI positive cell number percentage augmentation by 31.8 and 36.5 fold after 24 and 48 h, respectively for Rosc treatment. The increase was found 27.5 and 56 fold for the same time periods respectively after Pur treatment (Fig. 1d, bottom panel). Finally, we
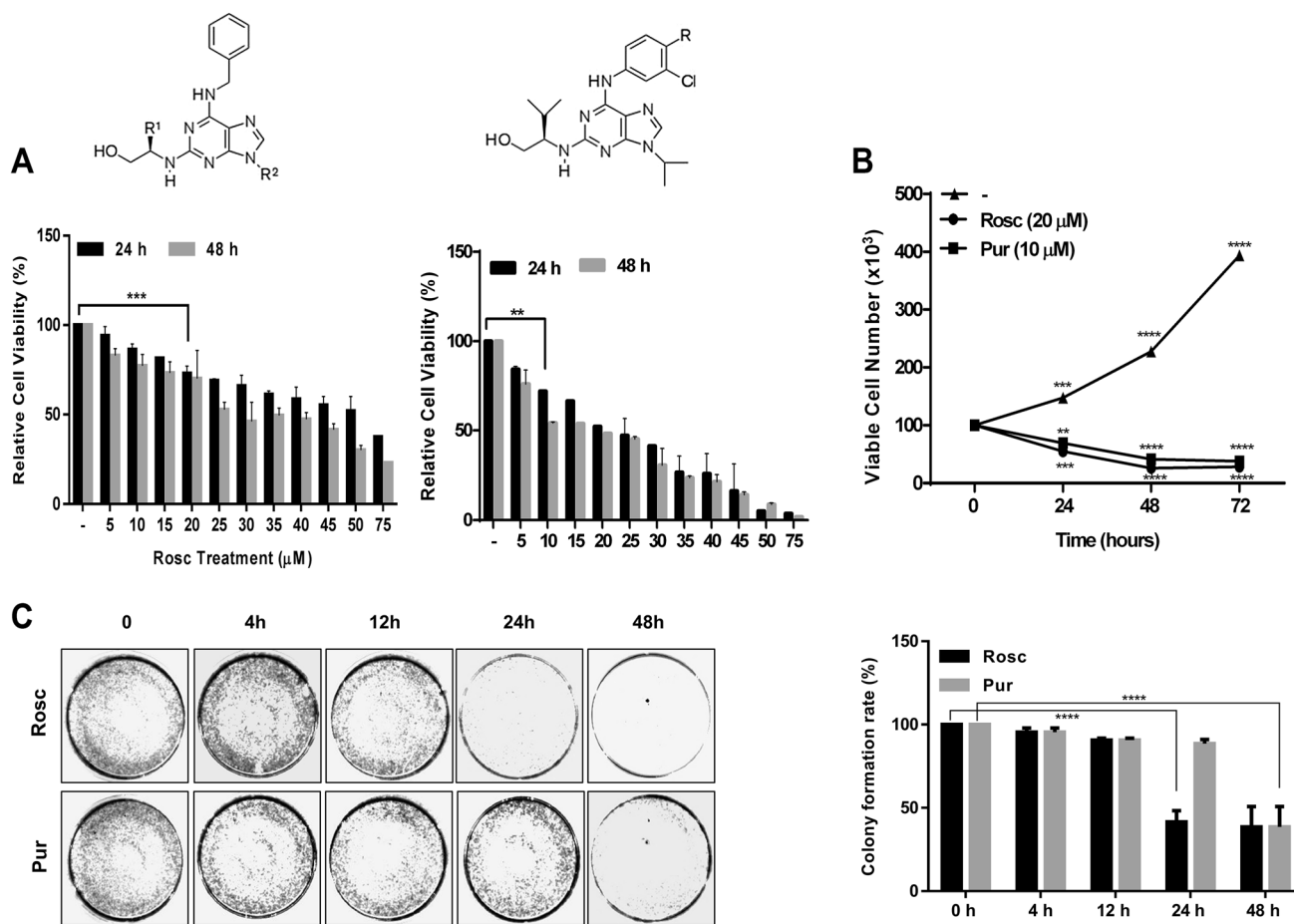

Fig. 1 Roscovitine and purvalanol decreased cell survival, proliferation and colony forming potential of HeLa cells. **a** The time and dose-dependent effect of Rosc and Pur on HeLa cell viability was determined by MTT assay. The experiment was analysed by two-way ANOVA and Tukey's multiple comparisons test. ***p < 0.0001, **p < 0.001. **b** Cell proliferation analysis with trypan blue dye exclusion assay showed that Rosc and Pur inhibited cell proliferation in time-dependent manner. Cell proliferation experiment was analysed by two-way ANOVA and Tukey's multiple comparisons test. **p < 0.001. **c** Rosc and Pur inhibited the colony formation of HeLa cells which was determined by colony formation assay. The rate of the colony formation was calculated according to pixel analysis using ImageJ software (left panel). **d** Cell death promoting role of Rosc and Pur was detected by PI staining fluorescence microscopy. The quantification of cell death was given as a bar graph for propidium iodide stained cells (left panel)
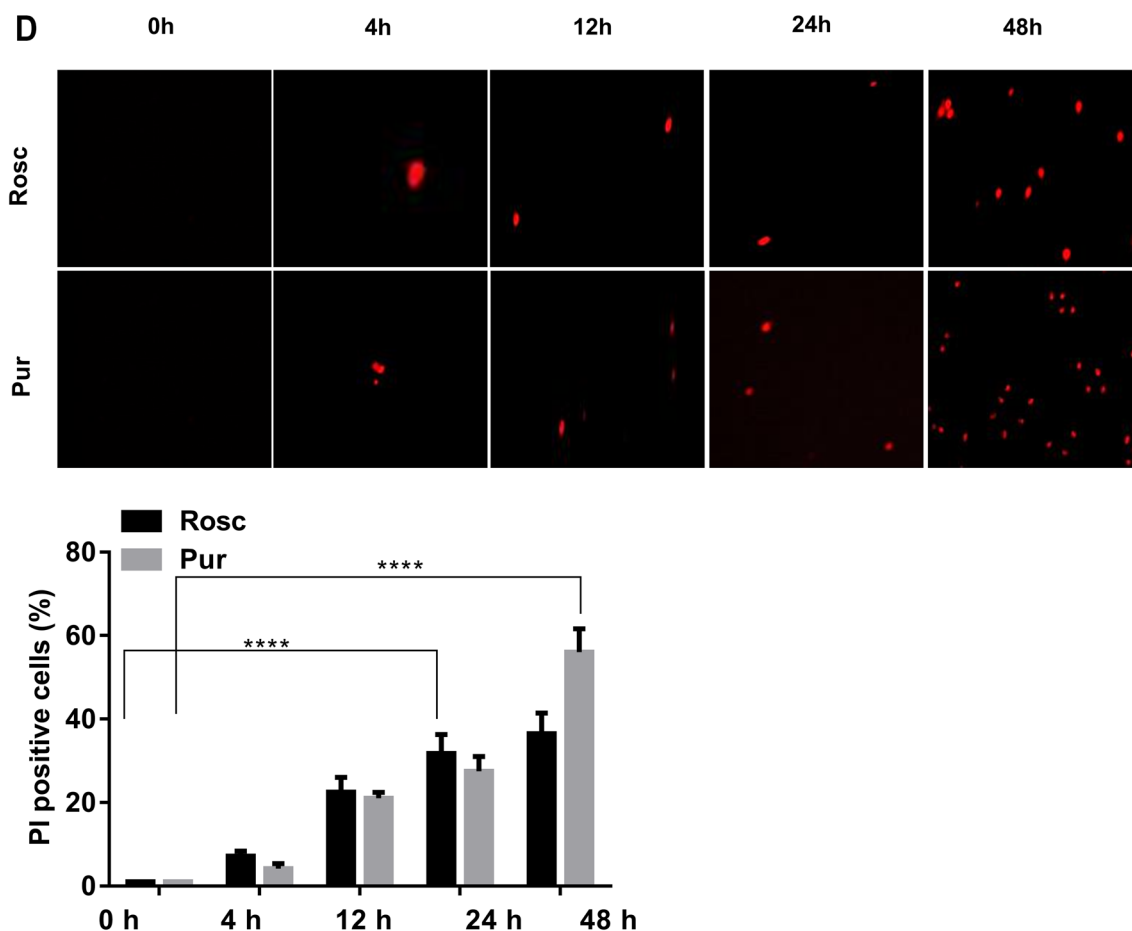
Fig. 1 (continued)

concluded that both CDK inhibitors were able to suppress cell survival at selected doses and induce cell death.

Roscovitine and purvalonol induced apoptosis through increasing cell cycle arrest and ROS generation

In order to determine the apoptotic efficacy of drugs at selected concentrations in HeLa cervical cancer cells, we first investigated the effect of Rosc and Pur on cell cycle phases by PI staining and read results with flow cytometry. Rosc increased the subG1 population in a time-dependent manner, more significantly following 48 h (5.3 fold vs. control). Rosc was also able to diminish S phase population percentage time-dependently, at 24 h the decrease was 1.7 fold compared to control samples. Similar to Rosc, Pur treatment triggered subG1 population increase by 5.5 fold compared untreated control samples as well. Unlike Rosc, Pur treatment caused G2/M arrest in HeLa cells. The G2/M population augmented by threefold compared to untreated HeLa cells (Fig. 2). To identify cell death mechanism in detail,

we performed Annexin V/PI staining and analyzed samples using flow cytometer. Rosc was effective to induce apoptotic population percentage in a time-dependent manner. As shown in Fig. 3a, in the first 24 h early apoptotic population ratio was increased. At 48 h, mostly late apoptotic population was observed (Fig. 3a). Pur treatment triggered early apoptotic population time-dependently; conversely, at 48 h time period necrotic cell percentage was increased (Fig. 3a). To confirm the apoptotic potential of each CDK inhibitors, we checked DNA fragmentation and MMP (mitochondrial membrane potential) disruption by DAPI and DiOC6 staining, respectively. Time-dependent Rosc and Pur treatment induced DNA fragmentation, a biomarker for apoptotic cell death, which was observed by nuclear blue dots following DAPI staining under fluorescence microscope (Fig. 3b, left panel). The cells with fragmented DNA significantly increased following 24 and 48 h with CDK inhibitors treatment (Fig. 3b, right panel). Next we investigated MMP after CDK inhibitors treatments in HeLa cells via DiOC6 staining. Both Rosc and Pur induced MMP loss that was observed by the decrease of green stained cells time-dependently
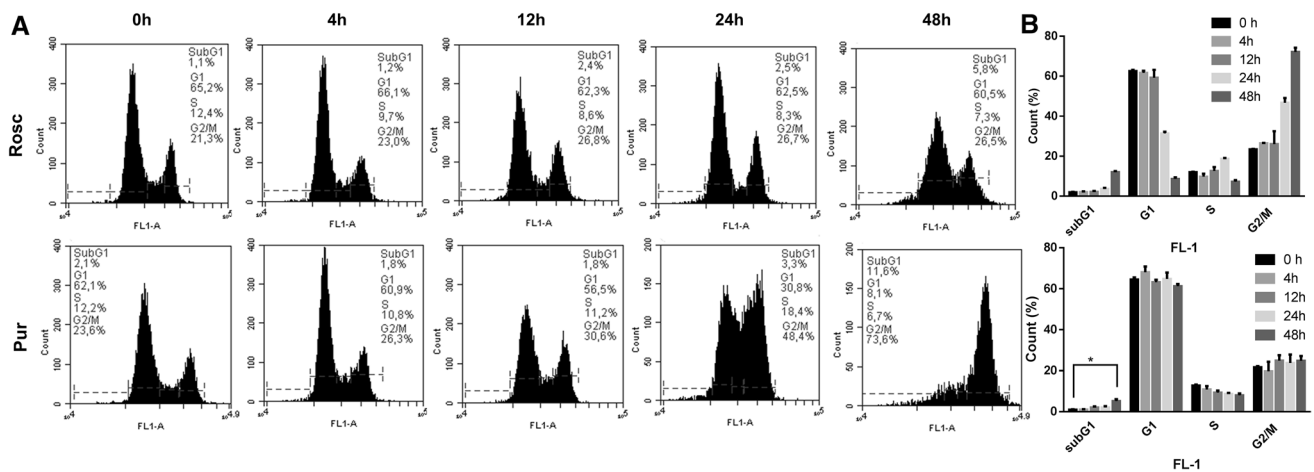
Fig. 2 Roscovitine and purvalanol induced G2/M accumulation in the cell cycle. **a** HeLa cells were treated for 4–48 h with Rosc and Pur. Propidium iodide (PI) staining and flow cytometry were used for cell cycle analysis (Ex: 535 nm and Em: 617 nm). Cell cycle distribution was analysed by two way ANOVA and Tukey's multiple comparisons test and *$p < 0.05$

(Fig. 3c, left panel). The decrease of MMP induced by Rosc and Pur for 24 and 48 h was found significant in HeLa cells (Fig. 3c, right panel). Finally, we also demonstrated that both CDK inhibitors were able to induce PARP cleavage time-dependently. Rosc triggered PARP cleavage starting from 12 h and this effect was very significant at 48 h (Fig. 3d). Similarly, Pur exerted a time-dependent PARP cleavage action (Fig. 3d). We also checked the PARP cleavage profile with the same CDK inhibitors concentrations starting from very early time points. Rosc and Pur induced apoptosis starting from 15′ treatment. While Rosc effect continued until 2 h, Pur treatment was less effective after 15′. However, PARP cleavage was significant at 4 h in HeLa cells (Fig. 3d).

Since apoptosis is related to increased ROS levels in cells, we investigated ROS generation following exposure of cells to CDK inhibitors. For this purpose, cells were stained with cell-permeable DCFH-DA following Rosc and Pur treatment in HeLa cells and analyzed with flow cytometer. As shown in Fig. 3e, f, both Rosc and Pur induced ROS generation time-dependently starting from 15′ and within 4 h of treatment.

CDK inhibitors modulated the expression profiles of ER stress members in time and drug dependent manner

To understand the mechanistic action of Rosc and Pur to increase ROS levels and apoptosis, we checked the expression profiles of significant ER regulator proteins by immunoblotting assay. First, we checked ER resident chaperone proteins CALR and PDI. CALR expression was downregulated in a time-dependent manner in Rosc-treated HeLa cells whereas PDI expression level dropped after Rosc exposure for 15′ and remained same for other early time

applications (30′-4 h) (Fig. 4a, left panel), except a slight upregulation in 1 h. Rosc treatment induced IRE1α and PERK up-regulation after 30′, until 1 h. After this time period both proteins down-regulated slightly (Fig. 4a, left panel). In accordance with this data, the downstream target of PERK, eIF2α was phosphorylated starting from 30′ and deactivated after 1 h (Fig. 4a). The phosphorylation of eIF2α usually causes the activation of ATF4, which in turn translocate to nucleus in order to start the expression of its target genes such as pro-apoptotic Bcl-2 family members. Since UPR activation could trigger decreased protein synthesis and growth arrest in G1 phase of cell cycle, we also investigated the early time CDK inhibitors treatment response for G1 checkpoint control proteins CDK4 and cyclin D1. As shown in Fig. 4a, both CDK4 and cyclinD1 were down-regulated following 30′ Rosc in HeLa cells. On the other hand, until 30′ CDK4 expression was found upregulated.

Later, we determined the expression profiles of the mentioned targets after time-dependent Pur treatment. In contrast to Rosc treatment, Pur induced the up-regulation of CALR expression, especially for 4 h (Fig. 4a, right panel). We determined a slight up-regulation in PDI expression until 1 h; though, this effect started to diminish after this time period for Pur treatment (Fig. 4a, right panel). Unlike Rosc, Pur treatment triggered a time-dependent increase in the expression of both IRE1α and PERK. Concomitantly, peIF2α expression increased right after 15′ following Pur treatment; nevertheless, after 15′ it was found slightly decreased starting 30′ till 4 h (Fig. 4a, right panel). The downstream target of peIF2α, ATF4, exhibited the similar expression trend (Fig. 4a, right panel). We also observed that Pur was able to decrease the expression profiles of CDK4 and cyclinD1, as well as Rosc (Fig. 4a, right panel).
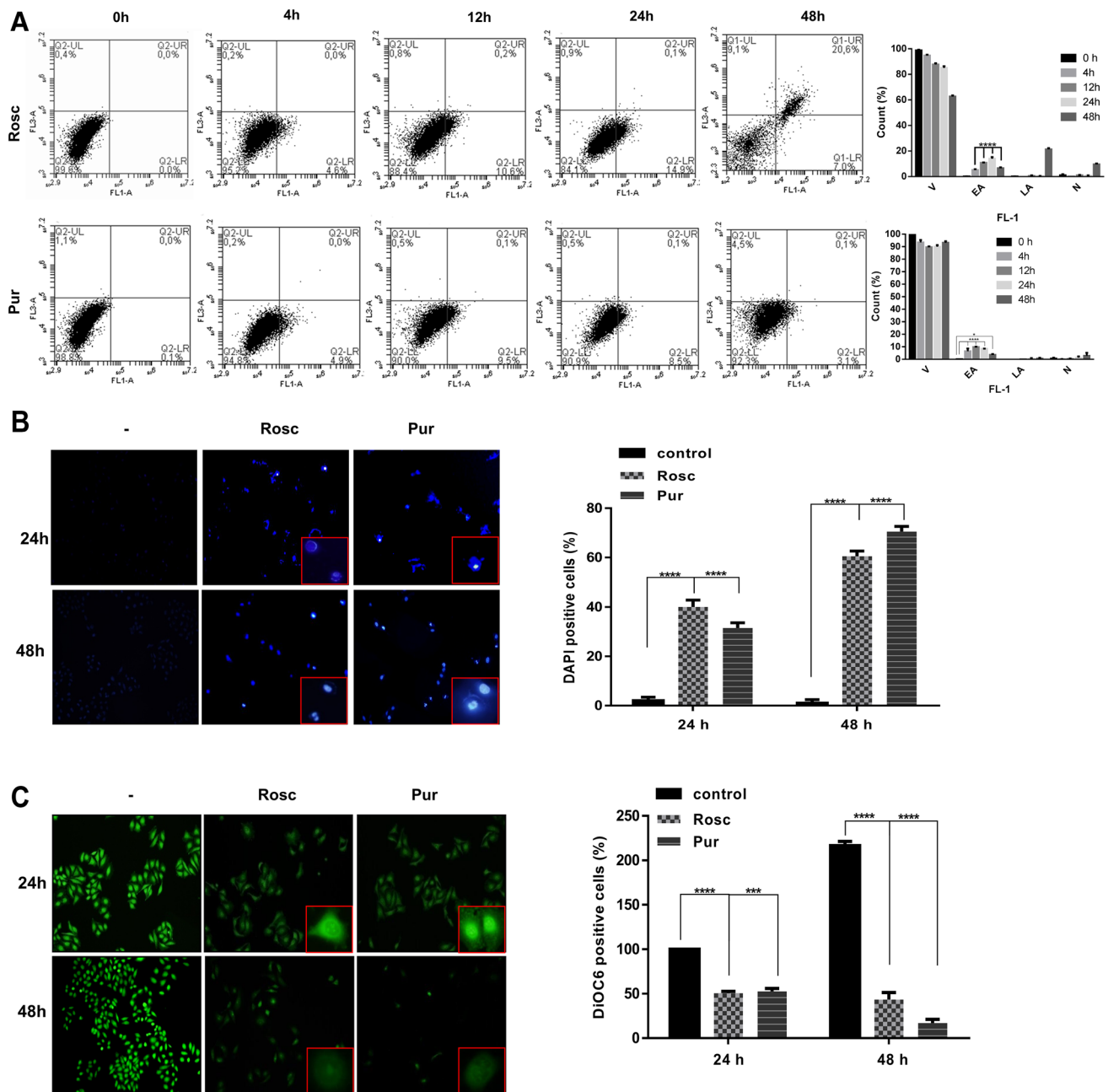
Fig. 3 Roscovitine and purvalanol induced apoptosis in time-dependent manner. **a** HeLa cells were treated with Rosc and Pur, stained with FITC-conjugated Annexin V/PI and subjected to flow cytometry. The lower left part represents viable cells, the lower right part represents early apoptotic cells, the upper left part represents necrotic cells and the upper right part represents secondary necrotic and late apoptotic cells. Annexin V/PI analysis performed by two way ANOVA and Dunnett's multiple comparisons test and $p < 0.0001$ was considered significantly different. *$p < 0.05$, ****$p < 0.0001$. **b** Determination of apoptosis by DAPI staining observed under fluorescence microscope following Rosc and Pur treatment in HeLa cells (Ex/Em: 358/461 nm). The quantification of DAPI stained apoptotic cells was

given as a bar graph (left panel). **c** MMP loss determined by DiOC6 staining following drug treatment under fluorescence microscope (Ex/Em: 482/504 nm). The quantification of DiOC6 stained cells was given as a bar graph (left panel). **d** Following time-dependent drug treatment, total proteins were isolated and separated on 12% SDS gel, transferred onto PVDF membranes and blotted with PARP and cleaved PARP antibodies. β-tubulin was used as a loading control. The effect of **e** Rosc and **f** Pur on ROS generation was determined by flow cytometry following DCFH-DA staining and analysed by two way ANOVA and Tukey's multiple comparisons test. *$p < 0.05$, ***$p < 0.001$, ****$p < 0.0001$
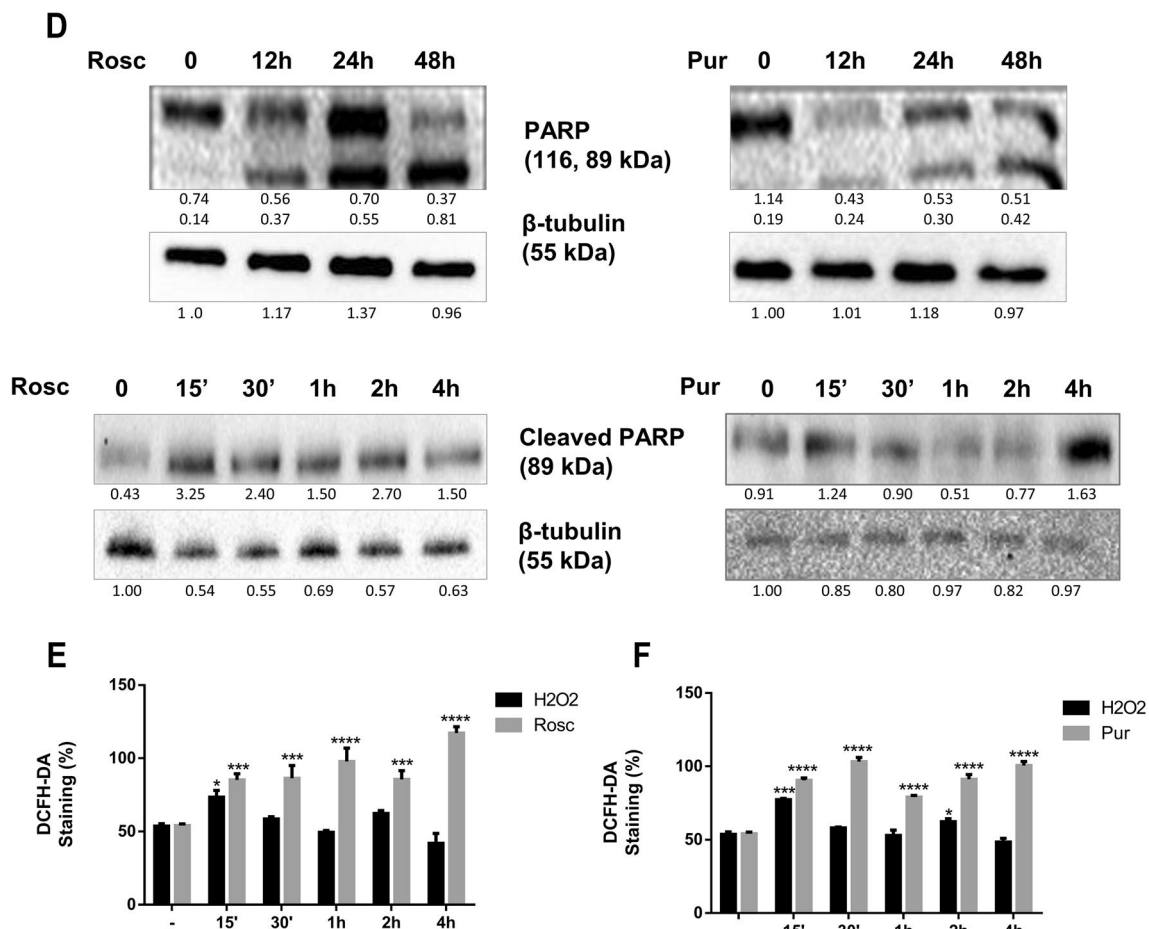
Fig. 3 (continued)

We next investigated the activation of CHOP during CDK inhibitors-mediated ER stress. For this purpose, we transfected cells with CHOP promoter (−649/+136) pmCherry-1 plasmid and determined the activation following drug treatment by FACS flow analysis. The optimization of transfection results were shown in Supplementary Fig. 1. Tunicamycin (10 µM) was used as a positive control to induce ER stress. Due to treatment with each CDK inhibitor, CHOP was activated in time-dependent manner (15′, 30′, 1, 2 and 4 h), in a similar way to tunicamycin treatment, compared to the untreated control group, resulting the puncta pattern in HeLa cells (Fig. 4b).

For the next step, we evaluated the expression profiles of the ER stress biomarkers in HeLa cells exposed to Rosc and Pur for late periods, 12–48 h. We found that Rosc was able to induce PDI in a time-dependent manner within 48 h (Fig. 4c, left panel). On the other hand, BiP expression was found significantly reduced in the first 12 h of Rosc treatment; conversely, after this time period the upregulation was lost and the expression came to the same level as control samples (Fig. 4c, left panel). Similar to PDI expression

alteration, the ER-membrane bound ER stress sensor IRE1α was upregulated in a time-dependent manner with Rosc treatment. In concordance with this data, the unspliced, inactive form of XBP1, which is a direct target of IRE1α, was found down-regulated (Fig. 4c, left panel). Rosc treatment caused increasing phosphorylation of eIF2α and ATF4 upregulation until 48 h. This effect diminished for both proteins when cells exposed to the drug for 48 h (Fig. 4c, left panel). Nevertheless, the downstream target of ATF4, CHOP is still active after 48 h, following a time-dependent increase within 24 h (Fig. 4c, left panel). We also assessed the ER stress players in response to Pur treatment in HeLa servical cancer cells. In a similar way to Rosc treatment, Pur was able to increase the expression profiles of both PDI and BiP within 48 h. IRE1α and eIF2α phosphorylation were found upregulated with time-dependent Pur, correlating with the decline in the expression of unspliced form of XBP1. In addition, Pur treatment increased ATF4 expression more effectively after 12 h, although the scenario was not the same for 24 and 48 h, the upregulation was still detectable for 24 and 48 h. HeLa cells also exhibited increased CHOP profile
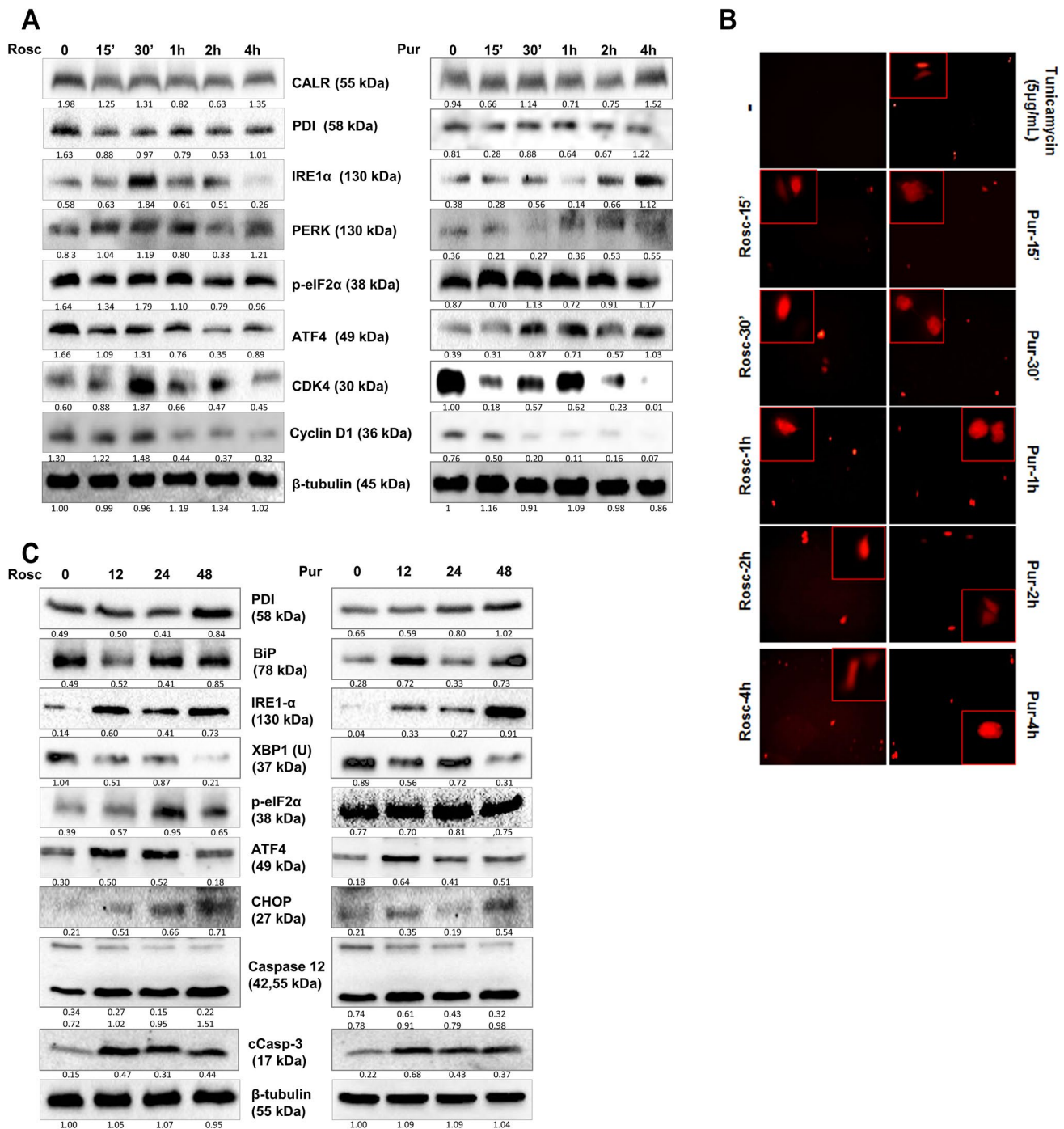
Fig. 4 Roscovitine and purvalanol induced ER stress in a time-dependent manner in HeLa cells. **a** After drug treatment, total proteins were isolated and separated on 12% SDS gel, transferred onto PVDF membranes and blotted with appropriate primary antibodies. β-tubulin was used as a loading control. **b** Cells were transfected with the reporter construct CHOP promoter (−649/+136) pmCherry-1. The CHOP activation due to drug treatment was visualized with fluorescence microscopy (Ex/Em: 575/601 nm). **c** Total proteins were isolated after 0–48 h drug treatment and separated on 12% SDS gel, transferred onto PVDF membranes and blotted with appropriate primary antibodies. β-tubulin was used as a loading control

after time-dependent Pur exposure. Since caspase 12 plays an important role in carrying-out the caspase-dependent UPR, we checked the effect of CDK inhibitors treatment on caspase-12 activation. Both Rosc and Pur were found effective time-dependently on caspase 12 cleavage (Fig. 4c). Upon activation of the UPR, caspase 12 translocates from

ER to the cytosol and start the caspase cascade via caspase 9 activation and caspase 3 cleavage. Our experiment set up clearly demonstrated activation of caspase 3 in time-dependent manner following both Rosc and Pur treatment (Fig. 4c).

## CDK inhibitors modulated autophagy response in HeLa cells

To determine the effect of Rosc and Pur on autophagy, we investigated the expression profiles of autophagy key players in time-dependent manner. Exposure of cells to each CDK inhibitors caused activation of autophagic response starting with the alterations in PDK-1 and Akt. The phosphorylation of PDK1 from Ser241, the site for Akt activation, was found increased after 12 and 24 h Rosc treatment, correlating with the increase in Akt expression levels (Fig. 5). However, PDK phosphorylation increased after 12 h slightly diminished in a time-dependent manner with Pur treatment (Fig. 5). The 12 and 24 h time points were found critical for Rosc treatment in HeLa cells since Beclin-1, Atg3 upregulations (Fig. 5). On the other hand, Pur treatment caused decrease in PDK1 phosphorylation at Ser241 residue with diminishing Akt expression (Fig. 5, right panel). Beclin-1 expression was upregulated at 12 and 24 h in a similar way to Rosc response in HeLa cells. Atg3, however, after a sharp expression increase following 12 h Pur treatment, started to downregulated slightly until 48 h.

Discussion

The cell cycle machinery is under control of CDKs with their substrates, cyclins, which are dysregulated during cancer progression [25]. Therefore, CDK targeting has been one of the anti-cancer strategies since decades. CDK inhibitors, Rosc and Pur have been shown to arrest cell cycle and

induce apoptosis in different cancer cell lines in vitro [26, 27]. Our aim was to investigate the apoptotic regulation related with ER stress process triggered by the CDK inhibitors. Our results suggested that both CDK inhibitors were effective to induce cell viability loss by 25% and inhibition in the survival rates following 20 μM Rosc and 10 μM Pur in HeLa cervical cells at 24 h. Our data were correlated with the latest reports on the effect of each CDK inhibitors on HeLa cells [6, 28, 29]. In addition, both CDK inhibitors abolished the colony formation potential of the cells in time-dependent manner, suggesting that Rosc and Pur are potential tumor growth inhibitors. Similar to our results, Rosc was suggested as a cell proliferation reducing agent in hormone therapy-resistant breast cancer cells as well as mouse hematopoietic progenitors both in vivo and in vitro [30, 31]. In addition, Pur was able to diminish tumor growth in Csk$^{-/-}$ c-Src cells, which are lack of Csk (C-terminal Src kinase) is responsible for the negative regulatory tyrosine phosphorylation of Src at Tyr-527 and as well as melanoma cell lines [32, 33]. Rosc and Pur treatments induced apoptotic cell death mechanism was demonstrated by different experimental set-ups such as PI and annexin V-PI double staining which showed that plasma membrane integrity of HeLa cells were abolished starting from 4 h of exposure, as well as a rapid mitochondria membrane hyperpolarization evidenced by the decrease in DiOC6 stained cells. DNA fragmentation visualized under fluorescence microscopy and PARP cleavage in a time-dependent manner both in early and late onset drug treatment confirmed the apoptotic induction of CDK inhibitors. In this quick responded cell-death process, we therefore investigated the involvement of ROS generation since the disruption in mitochondria membrane potential leads to efflux of ROS starting from the very early time intervals leading to increased Ca^{2+} levels, activated protein kinase cascades, global transcription reprogramming and rapid cell death [34]. We found that both Rosc and Pur

Fig. 5 Roscovitine and purvalanol induced autophagy in HeLa cells. Total proteins were isolated after drug treatment and separated on 12% SDS gel, transferred onto PVDF membranes and blotted with appropriate primary antibodies. β-tubulin was used as a loading control
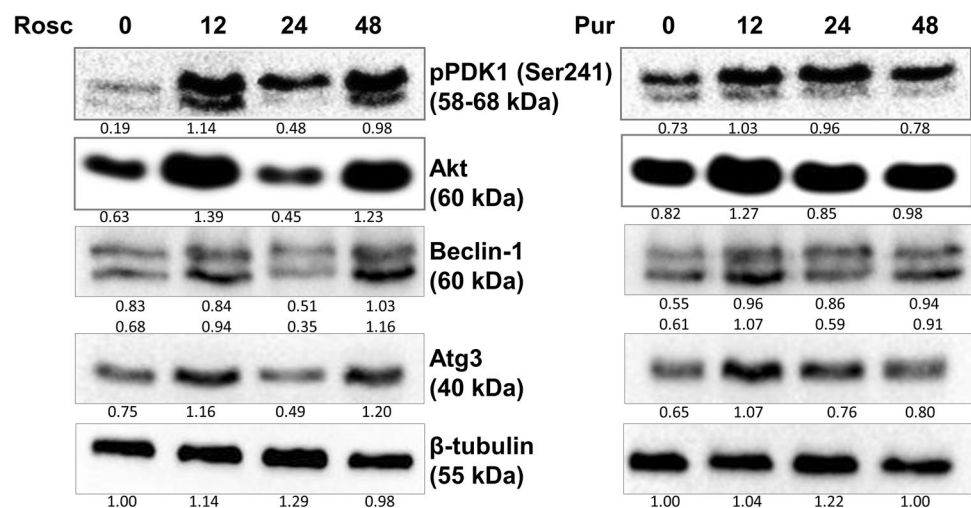
were able to increase ROS generation significantly when compared to untreated samples and H_2O_2 treated HeLa cells. These results also suggest that beginning from the early time point's mitochondrial depolarization occurred in response to CDK inhibitors and the depolarization continued until the end of 48 h, which was shown by DiOC6 staining. Our previous reports and other groups' publications also suggest that CDK inhibition increases ROS generation and ROS scavengers can prevent CDK inhibitors-induced apoptosis in different cell lines such as MCF-7, LNCaP, DU145, PC3 and HCT 116, breast, prostate and colon cancer cells, respectively [11, 35, 36].

The ER lumen environment designates the fate of entering proteins in terms of folding by PDI, CALR, glutathione (GSH)/glutathione disulfide (GSSG), NADPH oxidase 4 (Nox4), NADPH-P450 reductase (NPR) with calcium [37]. Evidences suggest that there is an interrelation of ER stress and ROS generation in cells due to these chaperones, which are redox-signaling mediators as well. During chaperone-mediated disulfide bond formation, electrons are provided to cysteines of the polypeptide chain from PDI active site leading to oxidation [38]. Therefore, during the folding process ER has been shown to generate ROS like mitochondria [39, 40]. ER is the main compartment responsible for the synthesis, folding and post-transcriptional modifications of proteins in eukaryotic cells. Appropriately, processed proteins are exported to the Golgi complex while incompletely folded ones are retained in the ER to complete the process or to be targeted for degradation. Any perturbations to these functions of ER, result in UPR and even cell death. The UPR coordinates the transcription of ER chaperones, the rate of protein synthesis and cell cycle [41, 42]. ER membrane stress sensors IRE1α, PERK and ATF6 make these regulations. Our results suggested that starting from the very early time point intervals, 30′ and 1 h, Rosc was able to induce ER stress via IRE1α and PERK. The upregulation in the downstream targets of PERK, ATF4 and p-eIF2α, were found correlating in terms of treatment time. On the other hand, Pur caused upregulation of IRE1α, PERK and its downstream targets more significantly after 2 h treatment in HeLa cells. Chaperones were found also affected by CDK inhibitors. Rosc induced the downregulation of CALR and PDI, while Pur upregulated CALR following 4 h and PDI after 1 h treatment. All these results suggest that both CDK inhibitors induced UPR starting different early time points. Our previous work has shown that exposure of HCT 116 colon cancer cells to Pur induced ER stress in a time-dependent manner via PDI and CALNX upregulation [11]. Our experiments also showed the time-dependent CDK4 and its partner cyclin D1 downregulation, which is expected response of HeLa cells to CDK inhibitors. On the other hand, recent reports also suggest that UPR response leads to accumulation of p27 and cell cycle arrest in different

cell lines. Therefore, decreasing effect might also be a part of UPR induction [43–46].

The enhanced expression levels of CHOP, one of the downstream targets of PERK and IRE1α, in response to CDK inhibitors also indicated that ER stress was induced in HeLa cells. CHOP has been described as an ER stress-mediated apoptotic inducer due to its transcription factor role for pro-apoptotic Bcl-2 family member Bim and repressor for anti-apoptotic Bcl-2 in response to ER stress inducers such as tunicamycin [47, 48]. In addition, CHOP-induced apoptosis was found closely related with suppression of cell cycle. The endogenous CDK inhibitor p21, when activated in response to a variety of stress conditions, has previously been suggested to be important in the transition of UPR from pro-survival to pro-apoptotic pathway. Therefore, Rosc and Pur treatment might cause the shift of UPR to the apoptosis with the crosstalk between cell cycle inhibition and the PERK/eIF2α/ATF4/CHOP pathway [49]. To understand the effect of both CDK inhibitors on prolonged ER stress, we checked the ER stress and apoptosis key players' expression profile in HeLa cells. We found that chaperones, PERK, IRE1α and its downstream targets are upregulated in a time-dependent manner starting from 12 h of treatment in response to both Rosc and Pur. We also showed that caspase-12, which is directly activated by Ca^{2+}-dependent calpains in response to ER stress, was activated after 12 h leading to the caspase-3 cleavage [50]. This data also demonstrated that CDK inhibitors induce ER stress-mediated apoptosis in HeLa cells.

Autophagy is a highly conserved process for the degradation of damaged organelles and un/mis-folded proteins in cells. It is controlled by a set of evolutionary conserved Atg proteins. Several studies demonstrated that autophagy has an important survival-promoting role in stress conditions [51, 52]. Recent publications showed that phosphorylation of eIF2α-ATF4-CHOP pathway contributes to autophagy activation induced by ER stress [47, 53]. Although autophagy is generally accepted as a tumor suppressor process to protect cancer cells from stress and present nutrient source, recent studies revealed that excessive self-degradation of cellular components essential for survival, such as mitochondria, causes cell death [54, 55]. In this context, CHOP has been shown as a responsible molecule to limit autophagy, induce apoptosis via upregulating Bim and suppressing Bcl-2 [56]. Our data indicated that Rosc and Pur were able to induce autophagy after 12 h treatment. Although this effect of Rosc abolished after 24 h, it was restored following 48 h. On the other hand, the autophagy response diminished in 24 and 48 h Pur treated HeLa cells.

Taken together, our study revealed that both CDK inhibitors were able to induce ER stress-mediated autophagy starting from early time points. After 12 h drug treatment cells died from apoptotic cell death, which was demonstrated
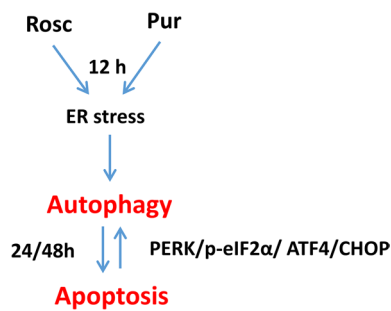
Fig. 6 The schematic representation of the CDK inhibitors

with PARP cleavage profile. Unlike Pur, Rosc treatment recovered autophagy related proteins after 48 h. Especially, PERK/p-eIF2α/ ATF4/CHOP pathway was found critical in CDK inhibitors-induced autophagy/apoptosis processes. All these findings could be important for the therapeutic potential and timing of CDK inhibitors against cervical cancer (Fig. 6).

Compliance with ethical standards

Conflict of interest The authors declare that they have no conflict of interest.

Ethical statement We declare that this article does not involve any studies with human participants or animals performed by any of the authors. The research has been performed on commercially available cell lines. All authors read and confirmed the final version of the manuscript.

References

1. Visagie MH, Jaiswal SR, Joubert AM (2016) In vitro assessment of a computer-designed potential anticancer agent in cervical cancer cells. Biol Res 49(1):43
2. Malumbres M, Barbacid M (2005) Mammalian cyclin-dependent kinases. Trends Biochem Sci 30(11):630–641
3. Bhattacharya S, Ray RM, Johnson LR (2014) Cyclin-dependent kinases regulate apoptosis of intestinal epithelial cells. Apoptosis 19(3):451–466
4. Whittaker SR, Te Poele RH, Chan F, Linardopoulos S, Walton MI, Garrett MD, Workman P (2007) The cyclin-dependent kinase inhibitor seliciclib (R-roscovitine; CYC202) decreases the expression of mitotic control genes and prevents entry into mitosis. Cell Cycle 6(24):3114–3131
5. Wesierska-Gadek J, Wandl S, Kramer MP, Pickem C, Krystof V, Hajek SB (2008) Roscovitine up-regulates p53 protein and induces apoptosis in human HeLaS(3) cervix carcinoma cells. J Cell Biochem 105(5):1161–1171
6. Coker-Gurkan A, Arisan ED, Obakan P, Ozfiliz P, Kose B, Bickici G, Palavan-Unsal N (2015) Roscovitine-treated HeLa cells finalize autophagy later than apoptosis by downregulating Bcl2. Mol Med Rep 11(3):1968–1974
7. Bach S, Knockaert M, Reinhardt J, Lozach O, Schmitt S, Baratte B, Koken M, Coburn SP, Tang L, Jiang T, Liang DC, Galons H, Dierick JF, Pinna LA, Meggio F, Totzke F, Schachtele C, Lerman AS, Carnero A, Wan Y, Gray N, Meijer L (2005) Roscovitine targets, protein kinases and pyridoxal kinase. J Biol Chem 280(35):31208–31219
8. Kolodziej M, Goetz C, Di Fazio P, Montalbano R, Ocker M, Strik H, Quint K (2015) Roscovitine has anti-proliferative and pro-apoptotic effects on glioblastoma cell lines: a pilot study. Oncol Rep 34(3):1549–1556
9. Gary C, Hajek M, Biktasova A, Bellinger G, Yarbrough WG, Issaeva N (2016) Selective antitumor activity of roscovitine in head and neck cancer. Oncotarget 7(25):38598–38611
10. Obakan P, Arisan ED, Ozfiliz P, Coker-Gurkan A, Palavan-Unsal N (2014) Purvalanol A is a strong apoptotic inducer via activating polyamine catabolic pathway in MCF-7 estrogen receptor positive breast cancer cells. Mol Biol Rep 41(1):145–154
11. Coker-Gurkan A, Arisan ED, Obakan P, Akalin K, Ozbey U, Palavan-Unsal N (2015) Purvalanol induces endoplasmic reticulum stress-mediated apoptosis and autophagy in a time-dependent manner in HCT116 colon cancer cells. Oncol Rep 33(6):2761–2770
12. Berrak O, Arisan ED, Obakan-Yerlikaya P, Coker-Gurkan A, Palavan-Unsal N (2016) mTOR is a fine tuning molecule in CDK inhibitors-induced distinct cell death mechanisms via PI3K/AKT/mTOR signaling axis in prostate cancer cells. Apoptosis 21(10):1158–1178
13. Obakan-Yerlikaya P, Arisan ED, Coker-Gurkan A, Adacan K, Ozbey U, Somuncu B, Baran D, Palavan-Unsal N (2017) Calreticulin is a fine tuning molecule in epibrassinolide-induced apoptosis through activating endoplasmic reticulum stress in colon cancer cells. Mol Carcinog 56(6):1603–1619
14. Rashid HO, Yadav RK, Kim HR, Chae HJ (2015) ER stress: Autophagy induction, inhibition and selection. Autophagy 11(11):1956–1977
15. Luo B, Lee AS (2013) The critical roles of endoplasmic reticulum chaperones and unfolded protein response in tumorigenesis and anticancer therapies. Oncogene 32(7):805–818
16. Deldicque L (2013) Endoplasmic reticulum stress in human skeletal muscle: any contribution to sarcopenia? Front Physiol 4:236
17. Cuervo AM (2004) Autophagy: in sickness and in health. Trends Cell Biol 14(2):70–77
18. Mizushima N, Klionsky DJ (2007) Protein turnover via autophagy: implications for metabolism. Annu Rev Nutr 27:19–40
19. Huang J, Dibble CC, Matsuzaki M, Manning BD (2008) The TSC1-TSC2 complex is required for proper activation of mTOR complex 2. Mol Cell Biol 28(12):4104–4115
20. McManus S, Bisson M, Chamberland R, Roy M, Nazari S, Roux S (2016) Autophagy and 3-phosphoinositide-dependent kinase 1 (PDK1)-related kinome in pagetic osteoclasts. J Bone Miner Res 31(7):1334–1343
21. He Q, Lee DI, Rong R, Yu M, Luo X, Klein M, El-Deiry WS, Huang Y, Hussain A, Sheikh MS (2002) Endoplasmic reticulum calcium pool depletion-induced apoptosis is coupled with activation of the death receptor 5 pathway. Oncogene 21(17):2623–2633

22. Yoshida T, Shiraishi T, Horinaka M, Wakada M, Sakai T (2007) Glycosylation modulates TRAIL-R1/death receptor 4 protein: different regulations of two pro-apoptotic receptors for TRAIL by tunicamycin. Oncol Rep 18(5):1239–1242

23. Wu Y, Fabritius M, Ip C (2009) Chemotherapeutic sensitization by endoplasmic reticulum stress: increasing the efficacy of taxane against prostate cancer. Cancer Biol Ther 8(2):146–152

24. Coker-Gurkan A, Arisan ED, Obakan P, Guvenir E, Unsal NP (2014) Inhibition of autophagy by 3-MA potentiates purvalanol-induced apoptosis in Bax deficient HCT 116 colon cancer cells. Exp Cell Res 328(1):87–98

25. Sutherland RL, Musgrove EA (2009) CDK inhibitors as potential breast cancer therapeutics: new evidence for enhanced efficacy in ER + disease. Breast Cancer Res 11(6):112

26. Appleyard MV, O'Neill MA, Murray KE, Paulin FE, Bray SE, Kernohan NM, Levison DA, Lane DP, Thompson AM (2009) Seliciclib (CYC202, R-roscovitine) enhances the antitumor effect of doxorubicin in vivo in a breast cancer xenograft model. Int J Cancer 124(2):465–472

27. Cihalova D, Hofman J, Ceckova M, Staud F (2013) Purvalanol A olomoucine II and roscovitine inhibit ABCB1 transporter and synergistically potentiate cytotoxic effects of daunorubicin in vitro. PLoS ONE 8(12):e83467

28. Wesierska-Gadek J, Borza A, Walzi E, Krystof V, Maurer M, Komina O, Wandl S (2009) Outcome of treatment of human HeLa cervical cancer cells with roscovitine strongly depends on the dosage and cell cycle status prior to the treatment. J Cell Biochem 106(5):937–955

29. Cui C, Wang Y, Wang Y, Zhao M, Peng S (2013) Exploring the relationship between the inhibition selectivity and the apoptosis of roscovitine-treated cancer cells. J Anal Methods Chem 2013:389390

30. Song H, Vita M, Sallam H, Tehranchi R, Nilsson C, Siden A, Hassan Z (2007) Effect of the Cdk-inhibitor roscovitine on mouse hematopoietic progenitors in vivo and in vitro. Cancer Chemother Pharmacol 60(6):841–849

31. Nair BC, Vallabhaneni S, Tekmal RR, Vadlamudi RK (2011) Roscovitine confers tumor suppressive effect on therapy-resistant breast tumor cells. Breast Cancer Res 13(3):R80

32. Du J, Widlund HR, Horstmann MA, Ramaswamy S, Ross K, Huber WE, Nishimura EK, Golub TR, Fisher DE (2004) Critical role of CDK2 for melanoma growth linked to its melanocyte-specific transcriptional regulation by MITF. Cancer Cell 6(6):565–576

33. Hikita T, Oneyama C, Okada M, Purvalanol A (2010) a CDK inhibitor, effectively suppresses Src-mediated transformation by inhibiting both CDKs and c-Src. Genes Cells 15(10):1051–1062

34. Rodic S, Vincent MD (2018) Reactive oxygen species (ROS) are a key determinant of cancer's metabolic phenotype. Int J Cancer 142(3):440–448

35. Franco J, Balaji U, Freinkman E, Witkiewicz AK, Knudsen ES (2016) Metabolic reprogramming of pancreatic cancer mediated by CDK4/6 inhibition elicits unique vulnerabilities. Cell Rep 14(5):979–990

36. Arisan ED, Obakan P, Coker-Gurkan A, Calcabrini A, Agostinelli E, Unsal NP (2014) CDK inhibitors induce mitochondria-mediated apoptosis through the activation of polyamine catabolic pathway in LNCaP, DU145 and PC3 prostate cancer cells. Curr Pharm Des 20(2):180–188

37. Zeeshan HM, Lee GH, Kim HR, Chae HJ (2016) Endoplasmic reticulum stress and associated ROS. Int J Mol Sci 17(3):327

38. Kramer B, Ferrari DM, Klappa P, Pohlmann N, Soling HD (2001) Functional roles and efficiencies of the thioredoxin boxes of calcium-binding proteins 1 and 2 in protein folding. Biochem J 357(Pt1):83–95

39. Walter P, Ron D (2011) The unfolded protein response: from stress pathway to homeostatic regulation. Science 334(6059):1081–1086

40. Zhong F, Xie J, Zhang D, Han Y, Wang C (2015) Polypeptide from Chlamys farreri suppresses ultraviolet-B irradiation-induced apoptosis through restoring ER redox homeostasis, scavenging ROS generation, and suppressing the PERK-eIF2a-CHOP pathway in HaCaT cells. J Photochem Photobiol B 151:10–16

41. Schroder M, Kaufman RJ (2005) ER stress and the unfolded protein response. Mutat Res 569(1–2):29–63

42. Bravo R, Parra V, Gatica D, Rodriguez AE, Torrealba N, Paredes F, Wang ZV, Zorzano A, Hill JA, Jaimovich E, Quest AF, Lavandero S (2013) Endoplasmic reticulum and the unfolded protein response: dynamics and metabolic integration. Int Rev Cell Mol Biol 301:215–290

43. Dkhissi F, Raynal S, Lawrence DA (1999) Altered complex formation between p21waf, p27kip and their partner G1 cyclins determines the stimulatory or inhibitory transforming growth factor-beta1 growth response of human fibroblasts. Int J Oncol 14(5):905–910

44. Han C, Jin L, Mei Y, Wu M (2013) Endoplasmic reticulum stress inhibits cell cycle progression via induction of p27 in melanoma cells. Cell Signal 25(1):144–149

45. Kitzmann M, Fernandez A (2001) Crosstalk between cell cycle regulators and the myogenic factor MyoD in skeletal myoblasts. Cell Mol Life Sci 58(4):571–579

46. Shenkman M, Tolchinsky S, Kondratyev M, Lederkremer GZ (2007) Transient arrest in proteasomal degradation during inhibition of translation in the unfolded protein response. Biochem J 404(3):509–516

47. Li Y, Guo Y, Tang J, Jiang J, Chen Z (2015) New insights into the roles of CHOP-induced apoptosis in ER stress. Acta Biochim Biophys Sin (Shanghai) 47(2):146–147

48. Tabas I, Ron D (2011) Integrating the mechanisms of apoptosis induced by endoplasmic reticulum stress. Nat Cell Biol 13(3):184–190

49. Mihailidou C, Papavassiliou AG, Kiaris H (2014) A crosstalk between p21 and UPR-induced transcription factor C/EBP homologous protein (CHOP) linked to type 2 diabetes. Biochimie 99:19–27

50. Rasheva VI, Domingos PM (2009) Cellular responses to endoplasmic reticulum stress and apoptosis. Apoptosis 14(8):996–1007

51. Chandrika BB, Yang C, Ou Y, Feng X, Muhoza D, Holmes AF, Theus S, Deshmukh S, Haun RS, Kaushal GP (2015) Endoplasmic reticulum stress-induced autophagy provides cytoprotection from chemical hypoxia and oxidant injury and ameliorates renal ischemia-reperfusion injury. PLoS ONE 10(10):e0140025

52. Zhang N, Ji N, Jiang WM, Li ZY, Wang M, Wen JM, Li Y, Chen X, Chen JM (2015) Hypoxia-induced autophagy promotes human prostate stromal cells survival and ER-stress. Biochem Biophys Res Commun 464(4):1107–1112

53. B'Chir W, Maurin AC, Carraro V, Averous J, Jousse C, Muranishi Y, Parry L, Stepien G, Fafournoux P, Bruhat A (2013) The eIF2alpha/ATF4 pathway is essential for stress-induced autophagy gene expression. Nucleic Acids Res 41(16):7683–7699

54. White E, DiPaola RS (2009) The double-edged sword of autophagy modulation in cancer. Clin Cancer Res 15(17):5308–5316

55. Kulkarni YM, Kaushik V, Azad N, Wright C, Rojanasakul Y, O'Doherty G, Iyer AK (2016) Autophagy-induced apoptosis in lung cancer cells by a novel digitoxin analog. J Cell Physiol 231(4):817–828

56. B'Chir W, Chaveroux C, Carraro V, Averous J, Maurin AC, Jousse C, Muranishi Y, Parry L, Fafournoux P, Bruhat A (2014) Dual role for CHOP in the crosstalk between autophagy and apoptosis to determine cell fate in response to amino acid deprivation. Cell Signal 26(7):1385–1391